Supplementary Text for "Limitations of collateral flow after occlusion of a single cortical penetrating arteriole"

N. Nishimura, N.L. Rosidi, C. Iadecola, and C.B. Schaffer

Supplementary Methods

Vascular identification

Penetrating arterioles were identified as vessels plunging into the brain in which the flow was directed into the brain parenchyma, as confirmed by using linescans in the surface segment of the penetrating vessel. Penetrating arterioles give rise directly to a capillary network. Communicating arterioles are defined as the surface arterioles that give rise to other arterioles and do not penetrate into the cortex. Subsurface vessels include penetrating arterioles, capillaries and ascending venules. The measured and targeted penetrating arterioles come from the same population, with similar diameters (11.7 μm mean diameter for targets and 11.9 μm for neighboring) and speeds (4.9 mm/s mean speed for target vessels and 4.7 mm/s for neighboring) (Supplementary Fig. 1). For convenience, we defined all the branches of penetrating arterioles of a size less than 10 μ m as "capillaries". Capillaries coalesced into ascending venules, defined as vessels that run vertically up to the cortical surface and in which flow is directed out of the cortex (Fig. 3a).

To quantify the topological relationship between the penetrating arteriole targeted for clotting and neighboring penetrating arterioles we counted the number of branches between the target and neighboring penetrating arterioles, as traced through the surface arteriole network. We also categorized capillaries by the number of branches they lie downstream from the penetrating arteriole that was targeted for occlusion. Capillaries with no connection to the target penetrating arteriole that could be traced in our image volume and capillaries more than 10 branches away from the target vessel were grouped together ("> 10 branches"). This latter group includes capillary branches from penetrating arterioles neighboring the occluded vessel. This quantification scheme was selected rather than conventions based on branching order or diameters (Jiang et al. 1994; Ley et al. 1986; Lipowsky 2005) because penetrating arterioles seem to serve a unique anatomical and topological position linking the two-dimensional surface arteriole network to the three-dimensional capillary bed. In addition, our previous studies have shown regardless of the type of vessel occluded (surface arteriole (Schaffer et al. 2006), capillary (Nishimura et al. 2006) or penetrating arteriole (Nishimura et al. 2007)) the number of branches a vessel sits away from the occlusion is a strong determinant of the amount of RBC speed change. The disadvantage of this scheme is that it does not facilitate comparison to other organs because it starts the count at anatomical features that are unique to the brain.

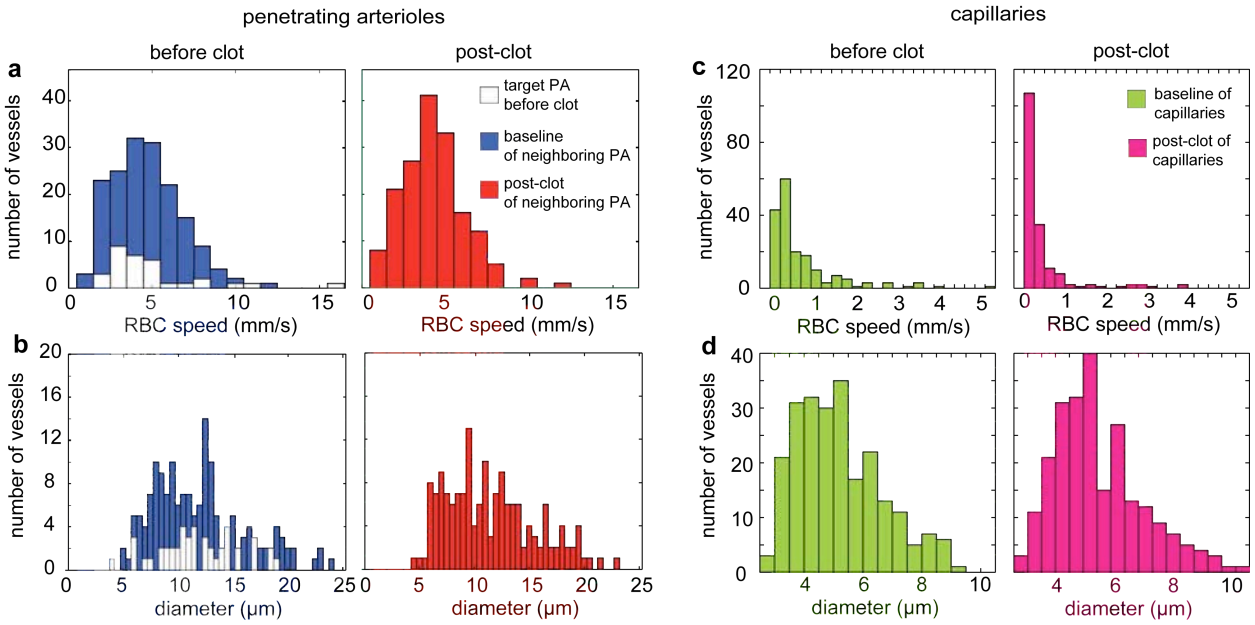

Supplementary Fig. 1. Histograms showing distributions of centerline red blood cell speeds (a) and vessel diameter (b) of targeted and measured penetrating arterioles (PA) before and after occlusion of the target vessel. These histograms include both urethane and isoflurane anesthesia and femtosecond and rose bengal occlusion methods. Histograms of capillary red blood cell speeds (c) and vessel diameters (d) before and after occlusion of a nearby penetrating arteriole.

Photothrombotic occlusion of penetrating arterioles

As an alternative to clotting with femtosecond laser ablation we used photochemical thrombosis. In this method, 1% (wt/vol) rose bengal in physiological saline was intravenously injected (100 mg/kg rat weight). While imaging with 2PEF microscopy, 1 mW of 532-nm wavelength laser light (Compass 215M; Coherent, Inc.) was focused on the lumen of the target vessel to photoactivate the rose bengal. The photoactivated rose bengal generates singlet oxygen, which locally damages the endothelium of the vessel and initiates clotting of the vessel (Sigler et al. 2008; Watson et al. 1985).

Plot generation

Box plots were generated with Matlab (Mathworks, Inc.) using the boxplot function which displays the 25th percentile value of the data set (first quartile), median, 75th percentile value of the data set (third quartile), and whiskers denoting the minimum and maximum values that are not outliers. Data points were considered outliers if points fell below the 1.5 times the interquartile range from the first quartile or above 1.5 times the interquartile range from the third quartile. The interquartile is defined as the third quartile minus the first quartile. Means were calculated excluding statistical outliers indicated by the box plot algorithm and are indicated as bold dots in the plots.

Trends with spatial distance away from target diving arteriole were analyzed using Matlab. A running median and 95% confidence interval with a 200-μm window was applied for arterioles (Fig. 2d-f), 50-μm window for capillaries (Fig. 4c-d). The median trend line and confidence

interval were then smoothed using a 50-μm wide moving average. Trend line points that were calculated with less than six data points were omitted from the graph. Matlab was used for k-means clustering analysis (Fig. 5b).

RBC flow determination in arterioles

Total flow in a vessel is the sum of plasma and RBC flow. Our measurements provide a direct assay of RBC speed, so we focus on a relationship for change in flow of RBCs, and do not consider plasma flow or changes in plasma flow. The RBC flow (volume of RBCs/time) in a vessel is related to radius, R, hematocrit, $h(r)$, and velocity, $v(r)$, which both vary with distance from the center of the vessel, r.

$$Flow_{RBC} = \int_0^R h(r)v(r)2\pi r dr \qquad \text{(Supplementary Eqn. 1)}$$

The RBC velocity profile across a small arteriole is not quite parabolic and varies over time with heartbeat. Previous measurements in rat brain arterioles of the shape of this profile averaged over time, however, suggest that approximating the RBC velocity profile as a function of r/R seems to be reasonable (Schaffer et al. 2006) because it is smooth and close to parabolic. The hematocrit profile across an arteriole *in vivo* is not well understood although measurements suggest that a cell free layer exists near the vessel wall, with RBCs packed closer to the vessel center. The hematocrit in this central region is a smooth function of radial position and is almost flat or slightly peaked in the center of the vessel (Aarts et al. 1988). These data suggest that both $v(r)$ and $h(r)$ are well-behaved functions that likely scale as r/R, so that the RBC flow is proportional to the area and v, the centerline speed of the vessel $Flow_{RBC} \propto R^2 v$. The proportionality constant depends on the flow profile and spatial variations in hematocrit.

In this work we present the ratios of RBC flow after a clot (or control) to the baseline value,

$$\frac{Flow_{RBC,post}}{Flow_{RBC,pre}} = \frac{R_{post}^{\ 2} v_{post}}{R_{pre}^{\ 2} v_{pre}} \qquad \text{(Supplementary Eqn. 2)}$$

so that we do not need to explicitly know the proportionality constant. We assume that any changes in diameter or speed in the vessel are small enough that the proportionality constant does not change. In the regime of the observed changes in diameters (~10%) and RBC speeds (~10%) in the arterioles measured in our work, neither the hematocrit distribution nor the shape of the RBC velocity profile in the same arteriole are likely to change enough to significantly alter the dependence RBC flow on area and centerline speed. Experimental data summarized by Furman and Olbricht (Furman and Olbricht 1985) suggest that the ratio between the average velocity of the RBCs and the flow of the combined plasma and RBCs is not strongly dependent on diameter in the range of the arteriole diameters studied here. This suggests that hematocrit distribution does not change dramatically in our experimental regime in arterioles and can be ignored in estimates the ratio of RBC flow, justifying the use of the relationship shown in Supplementary Eqn. 2.

The linescan velocity measurement technique was calibrated by translating fluorescently labeled, stationary samples on an encoded motorized stage. We estimate an uncertainty of 1% in the velocity measurement averaged over 40 s for vessels at 10 mm/s, at the upper range of speeds studied in this work. Because the position of edges of objects far apart (large separations compared to the diffraction-limited optical resolution) can be resolved to better than optical resolution of the microscope objective, we can resolve 0.25 μm changes in diameter, so for a 10-μm diameter vessel, 2.5% of diameter. Assuming that changes in flow scale as area x

speed this results in ~10% uncertainty in RBC flow. This is approximately the measured uncertainty found in repeated measurements of the same vessel (Schaffer et al. 2006) and is smaller than the flow changes reported in neurovascular coupling.

RBC flux and hematocrit measurement in capillaries

RBC flux (number of RBCs/time) was extracted from linescan data by explicitly counting the number of RBCs that pass through the vessel. This method works only in capillaries, where RBCs travel single file. For each time segment (43 ms) in the approximately 40-s long linescan data the angle of the streaks formed by moving RBCs was calculated and the image was rotated so that the lines are horizontal. The fluorescence intensity was then averaged along the horizontal direction. The edges between RBCs and the blood plasma were detected by thresholding at 15% of the maximum average intensity, and the number of RBCs was calculated as half the number of detected edges. This algorithm was verified with a comparison to a manual count of streaks formed by moving RBCs in the linescan images over approximately 2 seconds for 94 individual capillaries. We found that up to an RBC flux of approximately 50 RBC/s flux, the hand count and automated count agreed very well. At higher flux rates of 50-100 RBC/s, the automated count undercounted by about 30% so that our estimates of flux at baseline in faster flowing capillaries may be somewhat low.

To calculate the tube hematocrit in individual capillaries, we use the RBC flux determined above, together with the RBC speed and vessel size. To ensure accurate hematocrit measurements, we only evaluated vessels that at baseline had flux below 50 RBCs/s, where we found our RBC flux determination algorithm to be most accurate. This does mean that our data tends to exclude some of the faster vessels with higher flux. We use the average vessel radius across the segment in which the velocity and flux was measured. Following Constantinescu, *et al*, the capillary tube hematocrit, H_t, was calculated from the RBC flux, f, the RBC speed, v, the vessel radius, r, and volume of a red blood cell, V_{RBC} (Constantinescu et al. 2001). We used 55 μm^3 as the V_{RBC} for rat (Udden 2002).

$$H_t = \frac{fV_{RBC}}{v\pi r^2} \qquad \text{(Supplementary Eqn. 3)}$$

Supplementary Results

Lack of vasodilation in neighboring penetrating arterioles is independent of clotting method

We had some concern that the femtosecond laser ablation occlusion method might affect vasoactivity because this method causes some bleeding from the target vessel that could release vasoconstrictive factors. We used an alternate method based on clot initiation from endothelial damage resulting from singlet oxygen production by irradiation of intravenously injected rose bengal (Nishimura et al. 2007; Schaffer et al. 2006; Sigler et al. 2008; Watson et al. 1985). This method does not produce significant extravasation. We found no significant difference in diameter changes between the two clotting methods (Supplementary Fig. 2a, 2-way ANOVA of ranks, p = 0.4). The RBC speed change showed a tendency for rose bengal method to have faster RBC speeds (Supplementary Fig. 2b, 2-way ANOVA of ranks p = 0.02, with p = 0.0003 for effect from clot method). However this slight difference in speed did not translate to a major effect on RBC flow, where no significant differences were found (Supplementary. Fig. 2c, 2-way ANOVA on ranks, p = 0.1619).

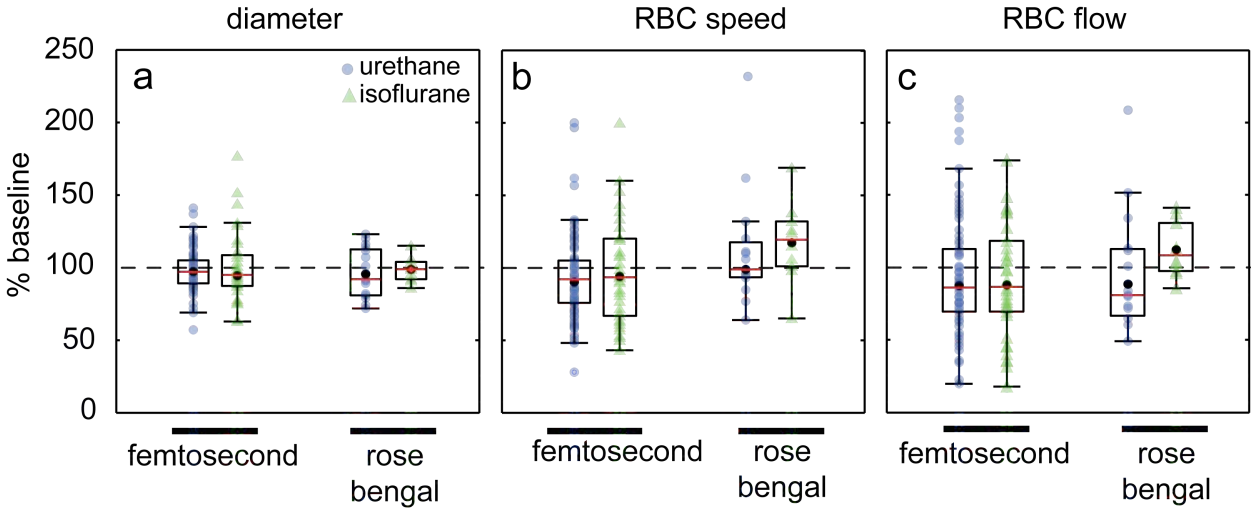

Supplementary Fig. 2. Occlusion technique dependence of diameter and blood flow changes in arterioles neighboring an occluded penetrating arteriole. Comparison of femtosecond laser ablation and rose bengal photochemical occlusion methods on diameter (a), centerline RBC speed (b), and RBC flow (c) after occlusion in penetrating arterioles, each expressed as percentage of baseline. Outliers not shown in (c) are 296% and 353% for the amplified technique, isoflurane anesthesia RBC flow measurements.

Hematocrit was unaffected in capillaries downstream from an occluded penetrating arteriole

Occluding a penetrating arteriole did not cause the capillary hematocrit to change relative to controls in either closely connected (four or fewer branches from occluded arteriole) or distantly connected vessels (Supplementary Fig. 3). Our measurements of capillary hematocrit in all capillaries was 39% +/- 16% (mean +/- std. dev.), which is higher than that found by other investigators who looked in cremaster preparations (~15%) (Constantinescu et al. 2001; Keller et al. 1994). Also, in brain both the RBC flux (55 +/- 40 RBC/s) and RBC velocities (0.78 +/- 0.46mm/s) tended to be much higher than that reported for cremaster (RBC flux ~10 RBC/s and capillary velocities ~0.1-0.2 mm/s) (Constantinescu et al. 2001; Keller et al. 1994), suggesting

organ-dependent differences in blood flow parameters account for the difference in hematocrit (Mchedlishvili et al. 2003).

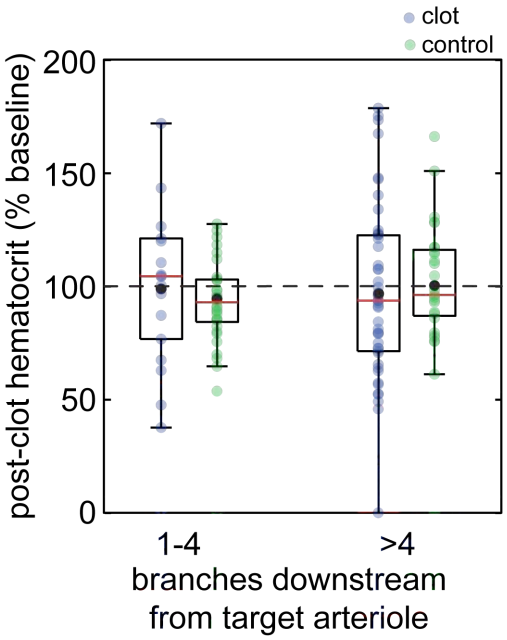

Supplementary Fig. 3. Capillary tube hematocrit did not change after penetrating occlusion. Post-clot capillary hematocrit, expressed as a percentage of baseline in capillaries after penetrating arteriole occlusion or time delay only (controls). Capillaries were grouped as closely connected (less than four branches downstream) or distantly connected (more than four branches downstream) to the target arteriole. No significant differences were detected with the Wilcoxon Mann Whitney rank sum test. One outlier is not shown (clot, 1-4 branches, 270%).

Relationship between topological and spatial distribution of capillaries

Capillaries were categorized as closely connected to a penetrating arteriole when there were four or fewer vascular branch points between the capillary and the penetrating arteriole. The remaining capillaries, which are five or more branches away from the arteriole, were categorized as distantly connected vessels. The division between closely and distantly connected vessels was based on clustering analysis of the physiological response of capillaries to an occlusion (Fig. 5b). In three animals, all visible capillaries (1101 vessels) within an imaging volume were categorized by the number of branches separating them from a targeted penetrating arteriole. The location of each capillary was reported as the position of the midpoint. About one third of the capillaries within 50 μm of the targeted arteriole are four or fewer branches downstream from the arteriole (closely connected). This fraction decreases over about 300 μm (Supplementary Fig. 4a). This decrease in the fraction of vessels that are closely-connected to a penetrating arteriole, and therefore slow after the arteriole is occluded, explains the increase in the average capillary speed with radial distance from the occluded vessel (black line in Fig. 4c and see Nishimura*, et al* (Nishimura et al. 2007).

Near a penetrating arteriole, a substantial fraction of the distantly connected capillaries have as their nearest neighbor a capillary that is closely connected (Supplementary Fig. 4b). The representation of the capillary network by the centerpoints of the vessels is only a first approximation and serves as an initial measure of the spatial relationship between capillaries.

Many capillaries wind great distances and will neighbor many vessels, so the nearest neighbor metric we use here tends to underestimate the degree of interactions between capillary territories. The closely connected capillaries are on average 46 +/-12 µm (mean +/- std) away from a distantly connected capillary (Supplementary Fig. 5a). A subset of distantly connected capillaries had a capillary that was closely connected to the target arteriole as the nearest neighbor. The average distance between these capillaries is 35 +/- 15 µm (Supplementary Fig. 5b).

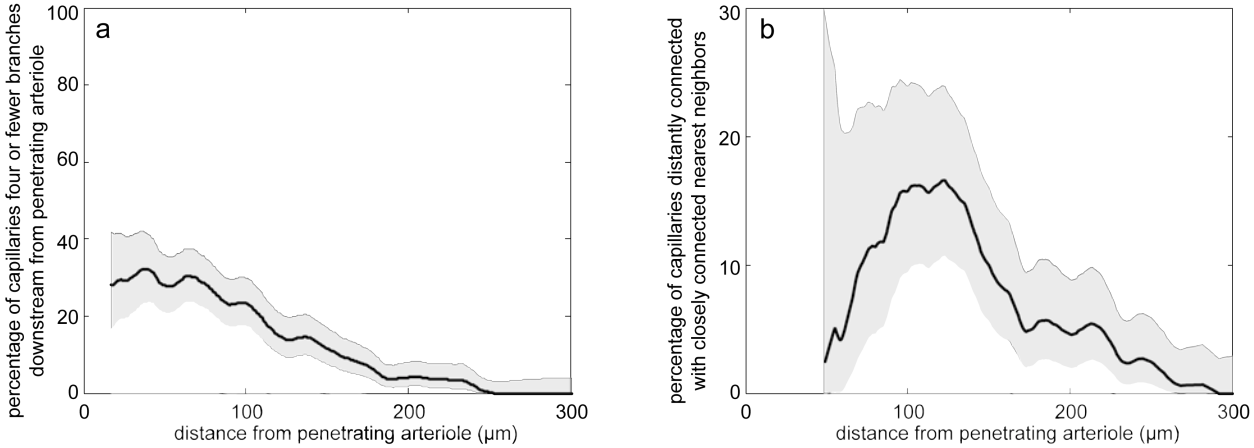

Supplementary Fig. 4. (a) Average fraction of vessels in a 50-µm moving window that are closely connected to a penetrating arteriole (less than four branches downstream) as a function of radial distance from the penetrating arteriole. (b) Average percentage of capillaries in a 50-µm moving window distantly connected to a penetrating arteriole (five or more branches) that have as their nearest neighbor a capillary that is closely connected to the penetrating arteriole (four or fewer branches). Gray shading indicates 95% confidence interval (binomial statistics). All traces were smoothed over 10 µm.

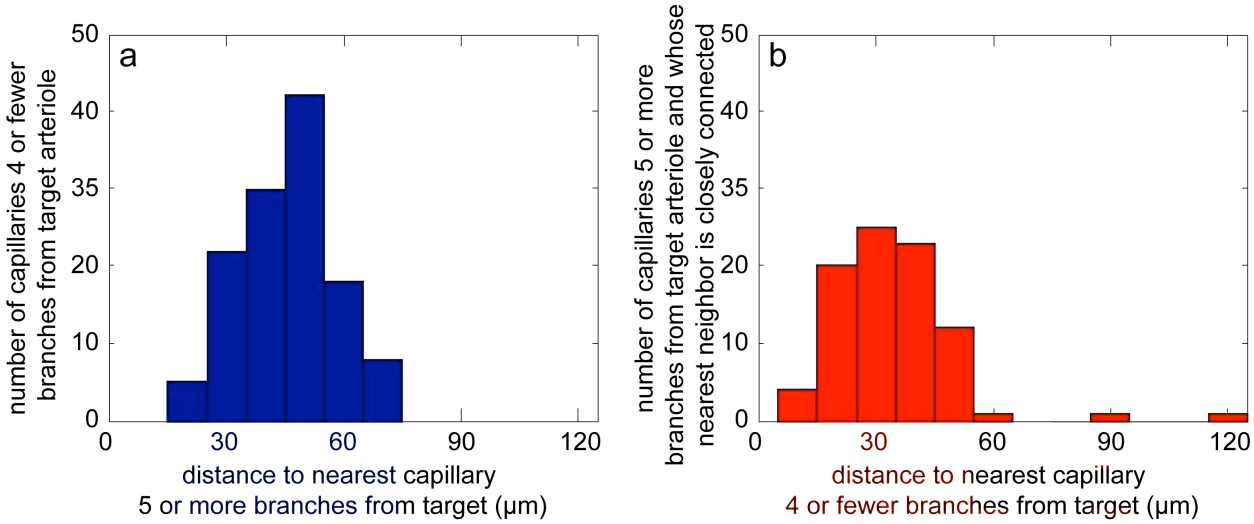

Supplementary Fig. 5. (a) Histogram of distances between closely connected capillaries and the nearest distantly connected capillary. (b) Histogram of distances between distantly connected capillaries and the nearest capillary for

the subset of distantly connected capillaries that had a capillary that was closely connected to the target penetrating arteriole as their nearest neighbor.

Red blood cell flux decreased in capillaries downstream from a penetrating arteriole occlusion

RBC flux was severely reduced in the first four capillary branches downstream from a penetrating arteriole occlusion (Supplementary Fig. 6), reflecting the same tendencies as the RBC speed (Fig. 6c). ACh application did not improve RBC flux in the closest branches (Supplementary Fig. 6). On average, across all measured capillaries the RBC flux was 55 +/-40 RBC/s, which matches previously measured values for brain (Kleinfeld et al. 1998; Villringer et al. 1994).

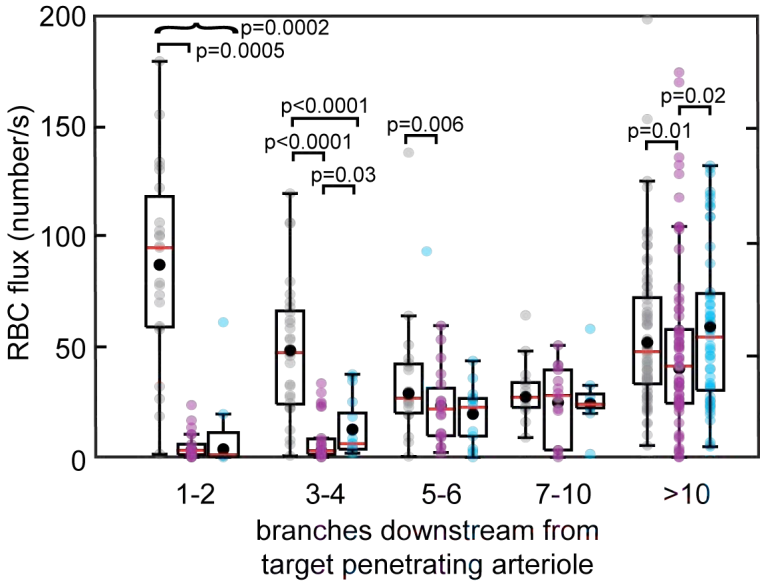

Supplementary Fig. 6. Flux dropped in downstream capillaries after penetrating arteriole occlusion. Flux in capillaries before, after clotting of a penetrating arteriole, and after ACh application as a function of the number of branches the capillaries are downstream from the occluded vessel. Square brackets indicate significant differences with Wilcoxon ranks sum test for paired data. Curly brackets indicate significant differences with Wilcoxon ranks sum test for unpaired data in one case in which not enough vessel pairs were measured for the paired test.

Post-hoc power analysis and sensitivity analysis

Our conclusion that there is no active arteriole compensatory response after the occlusion depends on observation of no vessel dilation. In order to estimate the probability of a Type II statistical error in which we have falsely concluded that there is no dilation, we conducted post-hoc sensitivity analysis. In this analysis we estimate the minimum change we should have been able to resolve given the number of measurements made and the measured variability in the data.

Arterioles after occlusion In arterioles, the most important data that supports our conclusion that there was no significant dilation in the neighboring penetrating arterioles is summarized in

Fig. 1f. For urethane, post-hoc analysis estimates the power of the study as 0.86. From sensitivity analysis we estimate that we should have been able to resolve a difference in change in diameters of 6.5% between the clot and control experiment with power = 0.95 and a 5% change with power = 0.8. We actually observed a reduction, rather than increase, in the mean vessel diameter of 6% in clot experiments relative to the controls, strongly suggesting there is no dilatory response in neighboring penetrating arterioles after occlusion of one penetrating arteriole. With isoflurane, the results have less power (0.15), but sensitivity analysis suggests that with power 0.95 (0.8), we would have be able to detect a difference of 16% (12%) allowing us to conclude that we do not expect that there is a change in diameter greater than about 15% relative to control. What further bolsters our confidence in the conclusion that there was no dilation is that after ACh was applied to the cortical surface the same vessels were remeasured and we detected a statistically significant dilation difference of 9% of baseline diameters between the clot and the ACh timepoints (Fig. 6a).

For all other measurements in arterioles the differences between clot and control groups were small enough that all powers were <0.8, which is consistent with the hypothesis that there is little change in the arterioles after the occlusion so that the effect size is very small. Using sensitivity analysis, we estimate the minimum changes our study was likely to detect. Both RBC speed and RBC flow dropped relative to baseline with a clot, supporting that idea that there is no extra perfusion that goes to the territories surrounding the occluded arteriole. With urethane anesthesia, sensitivity analysis leads us to expect to be able to resolve a 15% differences in RBC speed and RBC flow between clot and control groups with 0.80 power. We cannot rule out a smaller change in speed and flow. With isoflurane, with fewer measurements, we place the upper limit of resolvable change in RBC speed at 30% differences. For RBC flow with isoflurane, we estimate sufficient sensitivity to detect a 33% change. In all cases, the trends are consistent with no dilation and no increase in flow or speed in the surrounding penetrating arterioles. All means and medians for both urethane and isoflurane were lower than the controls. We also did not observe a significant difference in the behavior of communicating versus penetrating arterioles in diameter, speed or RBC flow (Fig. 2g-h). Sensitivity analysis estimates that we should have been able to resolve differences in vessel diameter changes of 12% with urethane between penetrating and communicating arterioles and 16% with isoflurane. In speed measurements and RBC flow calculations, communicating arteriole measurements had large variability, so we were unable to resolve differences less than about 50%. However, with both urethane and isoflurane, the speed and flow dropped relative to baseline, which is consistent with a lack of an active compensatory behavior.

Capillaries after occlusion We also claim to see no significant speed changes in capillaries distant (more than 4 branches) from the occluded arteriole (Fig. 4a). Post-hoc analysis estimates power for groups 5-6, 7-10 and 10+ to be low (< 0.35) due to high variability and sensitivity analysis suggests that we cannot make conclusions about the percentage change in speed. However, looking at the magnitude of the speeds (rather than normalized by baseline speeds) when comparing the RBC speed at baseline to that after the occlusion as in Fig. 6, powers in groups up to 10 branches are all greater than 0.9 and sensitivity analysis for group 7-10 suggests that we should have been able to detect a difference in RBC speed of 0.08 mm/s. In the group of capillaries greater than 10 branches away, the power is only 0.18 and we cannot rule out speed changes less than 0.2 mm/s. However, the trend across branches downstream from the occluded vessel argues strongly for a decreasing effect of the occlusion on speed with increasing topological distance. We also do not see a change in RBC speed between the post-clot measurement and the ACh application that reaches significance in most of the groups. Power is low in all branch groups, but we expected to be able resolve changes of 0.07 mm/s or less in all group up to 10 vessels away. In vessels more than 10 branches away, we cannot rule out changes less than 0.2mm/s and the trends suggest that there is actually an increase in RBC speed.

RBC flux in capillaries had similar trends to the speed (Supplementary Fig. 6). The data suggests that flux dropped in all groups of measured capillaries with the occlusion. ACh improved flow in some groups but not all. The power for the comparison of post-clot and ACh flux in group 1-2, 5-6, 7-10 is low <0.7 and sensitivity analysis suggests that we cannot rule out changes of less than 10 RBC/s.

We did not see significant dilation in capillaries five or more branches from the occluded arteriole relative to control (Fig. 4b). Power in the 5-6 branch group was 0.74, and we expected to be able to observe a 10% difference in changes in diameter relative to control with 0.80 power. In vessels 7-10 and more than 10 branches away power was <0.2, but we expected to be able to resolve difference in dilation of 12% and 3% respectively. The trend in the reduction of dilation with increasing branch numbers supports the idea that only the nearby vessels are affected.

We also do not see a change in capillary tube hematocrit with penetrating arteriole occlusion when compared to controls (Supplementary Fig. 3). For capillaries 1-4 branches downstream from the targeted penetrating arteriole, we would have expected to be able to resolve differences of about 16% between the clot and control. For capillaries more than 4 branches away, we expected to be sensitive to changes of 21%.

Captions for Additional Supplementary Files

Supplementary Table Physiological Monitoring
Physiological parameters were measured in most animals and values were averaged over each of the three stages of the experiment.
File format - pdf

Supplementary Data Tables
Tables corresponding to box plots showing median, mean, number of vessels, standard deviation and standard error of the mean for each column.
File format - pdf

Supplementary Movie
Three-dimensional rendering of vasculature shown in Fig. 3 using Voxx (Clendenon et al. 2002). The targeted penetrating arteriole was colored in red.
File format - mov

Supplementary References

Aarts PA, van den Broek SA, Prins GW, Kuiken GD, Sixma JJ, Heethaar RM. (1988) Blood platelets are concentrated near the wall and red blood cells, in the center in flowing blood. *Arteriosclerosis* 8:819-824

Constantinescu AA, Vink H, Spaan JA. (2001) Elevated capillary tube hematocrit reflects degradation of endothelial cell glycocalyx by oxidized LDL. *Am J Physiol Heart Circ Physiol* 280:H1051-1057

Furman MB, Olbricht WL. (1985) Unsteady Cell Distributions in Capillary Networks. *Biotechnology Progress* 1:26-32

Jiang ZL, Kassab GS, Fung YC. (1994) Diameter-defined Strahler system and connectivity matrix of the pulmonary arterial tree. *J Appl Physiol* 76:882-892

Keller MW, Damon DN, Duling BR. (1994) Determination of capillary tube hematocrit during arteriolar microperfusion. *Am J Physiol* 266:H2229-2238

Kleinfeld D, Mitra PP, Helmchen F, Denk W. (1998) Fluctuations and stimulus-induced changes in blood flow observed in individual capillaries in layers 2 through 4 of rat neocortex. *Proceedings of the National Academy of Sciences USA* 95:15741-15746

Ley K, Pries AR, Gaehtgens P. (1986) Topological structure of rat mesenteric microvessel networks. *Microvasc Res* 32:315-332

Lipowsky HH. (2005) Microvascular rheology and hemodynamics. *Microcirculation* 12:5-15

Mchedlishvili G, Varazashvili M, Kumsishvili T, Lobjanidze I. (2003) Regional hematocrit changes related to blood flow conditions in the arterial bed. *Clin Hemorheol Microcirc* 29:71-79

Nishimura N, Schaffer CB, Friedman B, Lyden PD, Kleinfeld D. (2007) Penetrating arterioles are a bottleneck in the perfusion of neocortex. *Proc Natl Acad Sci U S A* 104:365-370

Nishimura N, Schaffer CB, Friedman B, Tsai PS, Lyden PD, Kleinfeld D. (2006) Targeted insult to subsurface cortical blood vessels using ultrashort laser pulses: three models of stroke. *Nature Methods* 3:99-108

Schaffer CB, Friedman B, Nishimura N, Schroeder LF, Tsai PS, Ebner FF, Lyden PD, Kleinfeld D. (2006) Two-photon imaging of cortical surface microvessels reveals a robust redistribution in blood flow after vascular occlusion. *PLoS biology* 4:e22

Sigler A, Goroshkov A, Murphy TH. (2008) Hardware and methodology for targeting single brain arterioles for photothrombotic stroke on an upright microscope. *J Neurosci Methods* 170:35-44

Udden MM. (2002) In vitro sub-hemolytic effects of butoxyacetic acid on human and rat erythrocytes. *Toxicol Sci* 69:258-264

Villringer A, Them A, Lindauer U, Einhaupl K, Dirnagl U. (1994) Capillary perfusion of the rat brain cortex: An in vivo confocal microscopy study. *Circulation Research* 75:55-62

Watson BD, Dietrich WD, Busto R, Wachtel MS, Ginsberg MD. (1985) Induction of reproducible brain infarction by photochemically initiated thrombosis. *Annals of Neurology* 17:497-504